AADE-17-NTCE-108

A Comprehensive Hydraulic Software Package for Drilling Operations

Z. Ma, A. Karimi Vajargah*, A. Ambrus, P. Ashok, D. Chen, and E. van Oort, The University of Texas at Austin; R. May, D. Curry, J. Macpherson, and G. Becker, Baker Hughes

*Now with Quantum Reservoir Impact
Copyright 2017, AADE

This paper was prepared for presentation at the 2017 AADE National Technical Conference and Exhibition held at the Hilton Houston North Hotel, Houston, Texas, April 11-12, 2017. This conference is sponsored by the American Association of Drilling Engineers. The information presented in this paper does not reflect any position, claim or endorsement made or implied by the American Association of Drilling Engineers, their officers or members. Questions concerning the content of this paper should be directed to the individual(s) listed as author(s) of this work.

Abstract

Hydraulic modeling is an essential part of well construction planning. This task becomes even more crucial for drilling complex and challenging offshore wells with narrow drilling margins. However, the oil and gas industry still lacks a comprehensive transient hydraulic software package that can cover several advanced tasks such as conventional and dynamic well control, MPD and UBD design or testing sophisticated choke control algorithms, under one umbrella and without sacrificing much needed accuracy.

In this paper, we present a novel and comprehensive hydraulic software package and its underlying models. In addition to single-phase flow, this software can also model the transient multi-phase flow behavior of drilling fluid and influx/injected gas in the wellbore. The drift-flux approach was applied in association with appropriate closure relationships, sophisticated friction and choke models. Furthermore, a user-friendly graphical user interface was developed to ease the creation of simulation cases.

Through simulation scenarios, it will be shown that the new tool can accurately estimate several crucial parameters during well control such as the annular pressure profile, pump pressure, kick tolerance, flow out, pit gain or gas rising velocity, for any desired 3-D wellbore path. Applying advanced numerical schemes makes this tool fast, robust, efficient, and capable of simulating fast transients in drilling. As such, it has the potential to significantly improve well construction and drilling operations, thereby enhancing rig safety and reducing the associated non-productive time.

Introduction

One of the major tasks during the well construction process is hydraulic planning and predicting important parameters such as equivalent circulating density (ECD) and kick tolerance (during a gas kick). For this purpose, an accurate hydraulic model is required. The model should not only be applicable to conventional drilling operations but also be able to handle the complexities of more innovative drilling technologies such as underbalanced drilling (UBD) or managed pressure drilling (MPD). Regardless of the technology used, well control is a permanent concern in drilling operations. Precise estimation of key parameters associated with a well control scenario including the annular pressure profile, kick tolerance, bottom-hole and surface casing pressures or gas void fraction, plays a crucial role in the well construction process. However, common kick models used in industry consider a single bubble model while assuming the gas kick and the drilling fluid to remain in separate phases with simplifications regarding gas migration, frictional pressure loss or the length of the gas column. Due to these oversimplifications and the involved uncertainties, these models tend to produce very conservative results.

Another example includes the design of UBD operations in which steady-state two-phase empirical correlations are applied extensively (e.g. Beggs et al., 1973; Brill, 1985; Duns and Ros, 1963; Eaton et al., 1967; Hagedorn et al., 1965, etc.). These correlations are based on limited experimental data and are usually only applicable to Newtonian fluids. Hence, they are not necessarily valid for all simulation scenarios (Ma et al., 2016). In addition, they discard the slow transients associated with the UBD process, which makes the predictions even less reliable.

The most important goal of this paper is to introduce a comprehensive hydraulic model, which can cover a large variety of drilling operations under one umbrella rather than using a particular software for each operation, thereby aiding complex well design.

Background

Developing a realistic hydraulic model for drilling applications that include well control events is a very complicated process due to the existence of a complex multiphase region, which usually contains a non-Newtonian drilling fluid and formation / injected gas (Ma et al., 2016). Drill string movement and eccentricity also add to the complexity of the problem.

One major approach to model single-phase/multi-phase flow is using fundamental and mechanistic transport equations. Results obtained with this approach, which relies on the conservation of mass, momentum, and energy, are generally more reliable than the correlation-based models (Yuan and Zhou, 2009).

Depending on the simplifying assumptions, the mechanistic models can be classified into three categories: the homogenous model, the drift-flux model, and the two or multiple-fluid model. The transient drift-flux approach is applied in this study. The homogenous model with slippage between the phases is known as

the drift-flux model. In this model, in order to obtain the velocity of each phase, the so-called "slip law" has to be used in conjunction with the combined momentum equation (Gavrilyuk and Fabre, 1996; Rommetveit, 1989). The drift-flux model has been frequently reported in the literature for its usage in transient multi-phase flow modeling for drilling applications (Abouie et al., 2015; Avelar et al., 2009; Nickens, 1987; Podio and Yang, 1986; Rommetveit, 1989; Rommetveit and Vefring, 1991; Udegbunam et al., 2014). Although these simulators use the same drift-flux model concept, depending on the applied numerical schemes and slip laws, significantly different results may be obtained.

Two-fluid and multiple-fluid model is based on separated flow for each phase, where the slippage between the phases is considered via the interphase shear stresses. The two-fluid model needs one mass conservation equation and one momentum conservation equation for each phase (Bendiksen et al., 1991). Therefore, it is more computationally challenging. This model is also extensively used in the industry, particularly for production engineering applications (Abouie, 2015; Bendiksen et al., 1991; Shirdel and Sepehrnoori, 2012).

In comparison to the two-fluid model, the drift-flux model is simpler and less computationally expensive, which provided the main motivation for applying it in this study. Recent advances in developing numerical schemes, fluid flow modeling, and drilling techniques encouraged the development of a state of the art multiphase simulator for drilling and production applications.

Mathematical Model

In this section, a one-dimensional drift-flux mathematical model is proposed to describe the multi-phase flow dynamics. The model consists of conservation equations of mass and momentum for multiple gas and liquid components. In addition, closure algebraic equations including slip law, and choke model, are also presented.

Conservation Equations

The transient dynamics of multiphase flow can be modeled using conversation equations of mass and momentum as follows:

$$\partial_t A(x)\begin{bmatrix} \alpha_{l,i}\rho_{l,i} \\ \dots \\ \alpha_{g,k}\rho_{g,k} \\ \dots \\ \left(\sum_{i=1}^{I}\alpha_{l,i}\rho_{l,i}\right)v_l + \left(\sum_{k=1}^{K}\alpha_{g,k}\rho_{g,k}\right)v_g \end{bmatrix} + \tag{1}$$

$$\partial_x A(x)\begin{bmatrix} \alpha_{l,i}\rho_{l,i}v_l \\ \dots \\ \alpha_{g,k}\rho_{g,k}v_g \\ \dots \\ \left(\sum_{i=1}^{I}\alpha_{l,i}\rho_{l,i}\right)v_l^2 + \left(\sum_{k=1}^{K}\alpha_{g,k}\rho_{g,k}\right)v_g^2 + p \end{bmatrix} = A(x)\begin{bmatrix} q_{l,i} \\ \dots \\ q_{g,k} \\ \dots \\ f_w + f_G \end{bmatrix} \tag{2}$$

where equations (1) and (2) represents mass conservation of each liquid component and gas component, respectively. Equation (3) represents the momentum conservation of mixed liquid and gas components. The system contains I liquid components and K gas components. $\alpha_{l,i}$, $\rho_{l,i}$ are the volume fraction and density of the i^{th} liquid component. It is assumed that all liquid components share the same velocity v_l for a given location and time. Note that having two or more liquids with different properties is common in well control or cementing operations and has to be taken into consideration. $\alpha_{g,k}$, $\rho_{g,k}$ represent the volume fraction and density for the k^{th} gas component. Pressure p is common for all liquid and gas components. The cross-sectional area of the flow, A(x) may vary along the drill string due to area discontinuities (different wellbore, casing and drill string component sizes). $q_{l,i}$ and $q_{g,k}$ are the liquid/gas mass flow source/sink terms including reservoir gas influx, injected gas, lost circulation etc. f_w and f_G refer to the pressure drop caused by friction and gravity , respectively. The system has $2I + 2K + 3$ unknowns ($\alpha_{l,i}$, $\rho_{l,i}$, $\alpha_{g,k}$, $\rho_{g,k}$, v_l, v_g .and p) and $I + K + 1$ partial differential equations. The additional $I + K + 2$ algebraic equations are given by:

$$v_g = C_0 v_{mix} + v_d \tag{4}$$

$$\begin{cases} \rho_{l,i} = \rho_{l,i}(p,T) \\ \rho_{g,k} = \rho_{g,k}(p,T) \end{cases} \tag{5}$$

$$\sum_{i=1}^{I}\alpha_{l,i} + \sum_{k=1}^{K}\alpha_{g,k} = 1 \tag{6}$$

where equation (4) is the slip law describing the velocity difference between the gas and liquid phases. Equation (5) represents the density model of each gas or liquid component. Equation (6) indicates that the volume fractions of all liquid and gas components sum up to one.

Slip Law

Liquid and gas phases may have different velocities. The slip law describing the relation between gas velocity and liquid velocity is as follows:

$$\begin{cases} v_g = C_0 v_{mix} + v_d \\ v_{mix} = \left(\sum_{i=1}^{I}\alpha_{l,i}\right)v_l + \left(\sum_{k=1}^{K}\alpha_{g,k}\right)v_g \end{cases} \tag{7}$$

where C_0 is the concentration profile parameter and v_d is the drift velocity (also known as "slip velocity" or "gas rising velocity"). C_0 and v_d are empirical parameters and can be obtained from the available correlations (Roumazeilles et al., 1996; Oddie et al., 2003; Shi et al., 2005). Additional information about the slip law and choke models is presented in the Appendix.

Numerical Scheme

It is impractical to find an analytical solution to the presented drift-flux model due to the complexity of the underlying coupled partial differential equations and nonlinear algebraic equations. Instead, a numerical scheme could be applied to approximating the solution. In this paper, a second-

order semi-implicit relaxed scheme presented by Evje and Fjelde (2002) is modified to predict the solution. The scheme is modified to be able to handle a system of multiple liquid/gas components. The concept of energy conservation is used to handle the area discontinuities in the drill string and annulus.

Modified Second Order Relaxed Scheme

The second order relaxed scheme is briefly discussed in this section. The conservation equations in (1), (2) and (3) can be written as:

$$\partial_t U + \partial_x (F_c + F_p) = Q \tag{8}$$

where

$$U = \begin{bmatrix} U_m \\ U_M \end{bmatrix}, U_m = \begin{bmatrix} \alpha_{l,i}\rho_{l,i} \\ \dots \\ \alpha_{g,k}\rho_{g,k} \\ \dots \end{bmatrix},$$

$$U_M = \left(\sum_{i=1}^{I} \alpha_{l,i}\rho_{l,i}\right) v_l + \left(\sum_{k=1}^{K} \alpha_{g,k}\rho_{g,k}\right) v_g$$

$$F_p = \begin{bmatrix} 0 \\ \dots \\ 0 \\ \dots \\ p \end{bmatrix}, F_c = \begin{bmatrix} F_{mc} \\ F_{Mc} \end{bmatrix}, F_{mc} = \begin{bmatrix} \alpha_{l,i}\rho_{l,i}v_l \\ \dots \\ \alpha_{g,k}\rho_{g,k}v_g \\ \dots \end{bmatrix},$$

$$F_{Mc} = \left(\sum_{i=1}^{I} \alpha_{l,i}\rho_{l,i}\right) v_l^2 + \left(\sum_{k=1}^{K} \alpha_{g,k}\rho_{g,k}\right) v_g^2$$

$$Q = \begin{bmatrix} Q_m \\ Q_M \end{bmatrix}, Q_m = \begin{bmatrix} q_{l,i} \\ \dots \\ q_{g,k} \\ \dots \end{bmatrix}, Q_M = f_w + f_G$$

where U_m, U_M, F_{mc}, F_{Mc}, F_p, Q_m and Q_M are the mass conservative variables, momentum conservative variable, mass convective fluxes, momentum convective flux, pressure flux, mass source terms, and momentum source terms, respectively. As shown in **Figure 1**, the drill pipe and annulus are discretized into N cells. Each cell j consists of a node j at its center, a lower interface, $j - 1/2$, and an upper interface, $j + 1/2$. A relaxed scheme presented by Evje and Fjelde (2002) has been modified to solve the discretized system with multiple liquid/gas components:

$$\begin{cases} U_{m,j}^{(n+1)} = U_{m,j}^{(n)} + \dfrac{\Delta t}{\Delta x}\left[F_{mc,j-\frac{1}{2}}^{(n)} - F_{mc,j+\frac{1}{2}}^{(n)}\right] + Q_{m,j}^{(n)}\Delta t \\ U_{M,j}^{(n+1)} = U_{M,j}^{(n)} + \dfrac{\Delta t}{\Delta x} \times \\ \left[F_{Mc,j-1/2}^{(n)} - F_{Mc,j+\frac{1}{2}}^{(n)} + p_{j-\frac{1}{2}}^{(n+1)} - p_{j+\frac{1}{2}}^{(n+1)}\right] + Q_{M,j}^{(n)}\Delta t \end{cases} \tag{9}$$

where superscript (n) and $(n + 1)$ refer to the current and next time layer, respectively. Δt and Δx are the size of time step and the size of cell j, respectively. The selection of Δt and Δx must satisfy the CFL constraints for numerical stability. More details of the scheme can be found in (Evje and Fjelde, 2002).

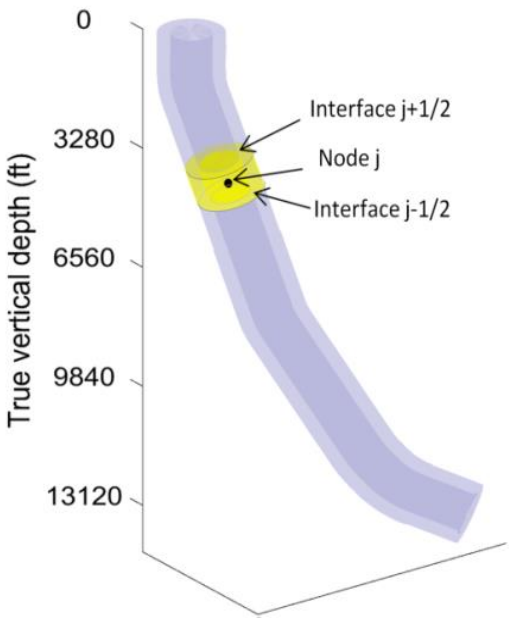

Figure 1 - System discretization.

Area Discontinuity Treatment

The presented numerical scheme cannot be directly applied to area discontinuities. A uniform mesh throughout the model geometry may result in irregular cell around the area discontinuities. Additionally, momentum is not conserved at the area discontinuities due to internal force. For this purpose, the discretization and scheme must be modified.

In this paper, cell interfaces are placed exactly on the area discontinuities. A uniform mesh is adopted within each segment separated by area discontinuities. Hence, the presented numerical scheme can be applied within each segment. The area discontinuity provides boundary conditions for the adjacent segments. As shown in **Figure 2**, a virtual cell with zero volume is considered at the discontinuity location. Since momentum is not conserved for the virtual cell, an energy conservation equation is used instead:

$$\begin{aligned} &\partial_t A\left(\sum_{i=1}^{I} \alpha_{l,i}\rho_{l,i}E_{l,i} + \sum_{k=1}^{K} \alpha_{g,k}\rho_{g,k}\,E_{g,k}\right) + \\ &\partial_x A\left(\sum_{i=1}^{I} \alpha_{l,i}\rho_{l,i}H_{l,i}v_l + \sum_{k=1}^{K} \alpha_{g,k}\rho_{g,k}\,H_{g,k}v_g\right) = 0 \end{aligned} \tag{10}$$

where E and H represent the specific energy and enthalpy, respectively. Numerical schemes have been developed for solving equations (1), (2) and (10) over the virtual cell, which provides boundary conditions for the adjacent segments.

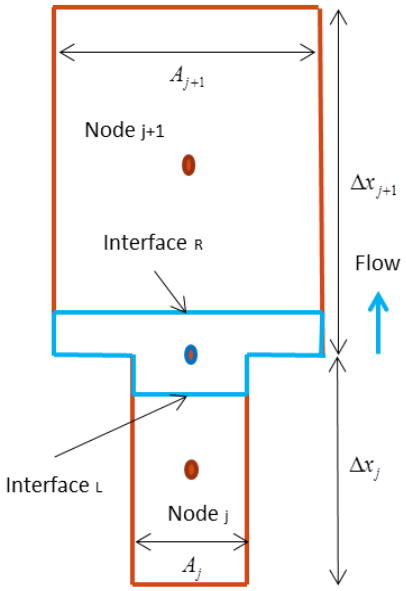

Figure 2 - Illustration of area discontinuity treatment.

Software Package

A software package has been developed based on the presented model. The software package can handle the following complexities:

- Arbitrary wellbore path
- Area discontinuities in wellbore or drill string
- Off-bottom drill string
- Advanced slip models
- Non-Newtonian drilling fluids
- Simultaneous existence of multiple types of liquid and gas components
- Real gas model
- Multiple influxes from several formations or injections
- Lost circulation due to fracture
- Advanced model for two-phase pressure drop across the bit and choke
- Automated choke control
- Modern drilling techniques such as MPD and UBD

Figure 3 shows the developed graphical user interface (GUI) for this software package. The user-friendly nature of the GUI allows the user to conveniently configure/import the model parameters and interactively simulate different drilling scenarios such as introducing an influx during simulations by selecting a reservoir pressure higher than the circulating wellbore pressure.

Model Validation

Simulation results from Evje and Fjelde (2002) are used to validate the numerical scheme applied in this study. Liquid and gas were pumped together from one end of a horizontal pipeline. The pipeline has a length of 1000 m and a diameter of 10 cm.

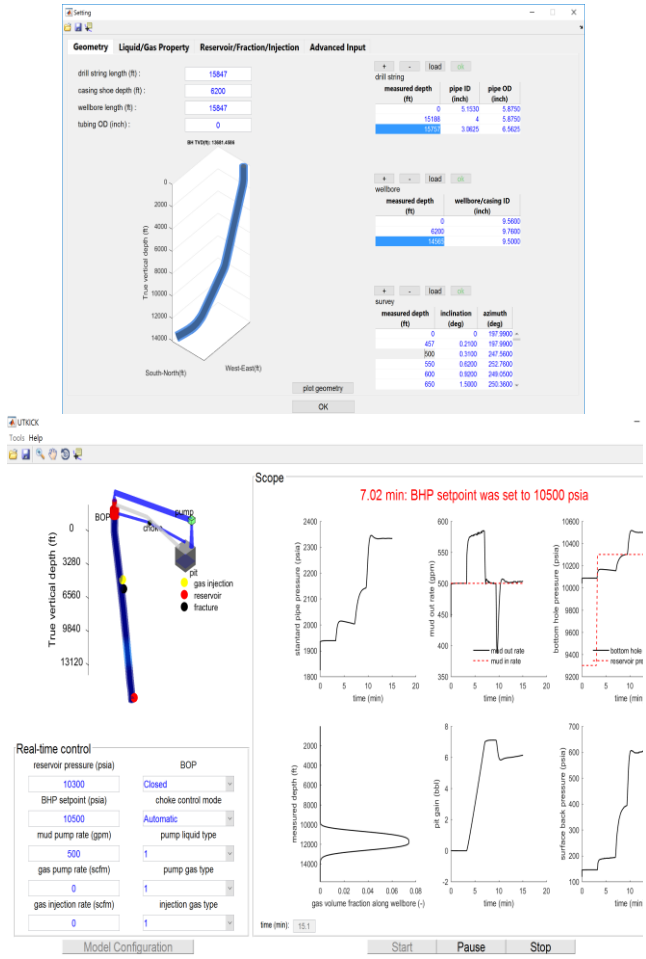

Figure 3 - Snapshot of the developed GUI for this software package: (top) example of model configuration; (bottom) example of interactive control user interface.

The liquid has a reference density of 1000 kg/m^3 and a constant viscosity of 0.05 Pa.s. The gas has a constant viscosity of 5×10^{-6} Pa.s. The speed of sound in liquid and gas were assumed to be 1000 m/s and 316 m/s, respectively. No slip was assumed between liquid and gas phases. The gas and liquid mass flow rates were increased to 0.02 kg/s and 3.0 kg/s in 10 s. The pressure at the outlet of the pipeline was kept constant at 1 bar. The gas volume fraction and pressure profiles at different times are shown in **Figure 4** and **Figure 5**. The solid lines represent the results on a fine grid. The dotted lines represent results on a grid with 50 cells. The results converge with increasing resolution, which is consistent with the results presented by Evje and Fjelde (2002).

Simulation Results

The software package is capable of simulating different well control cases including MPD, UBD, Driller's Method, Wait & Weight Method, etc. Simulations and validations of MPD scenarios have been shown in our previous work (Ma et al., 2016). Additional capabilities of handling multiple liquids and

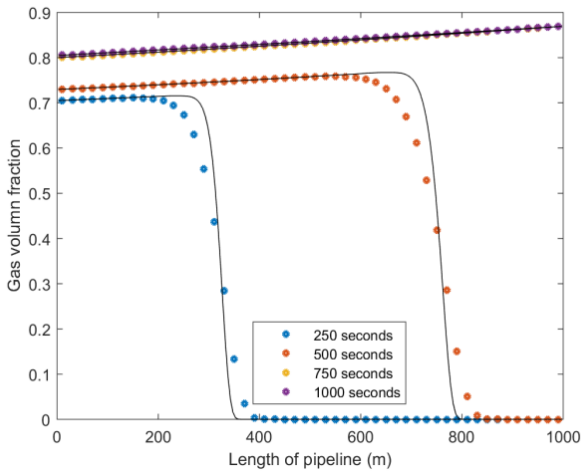

Figure 4 – Gas volume fraction profile at different times.

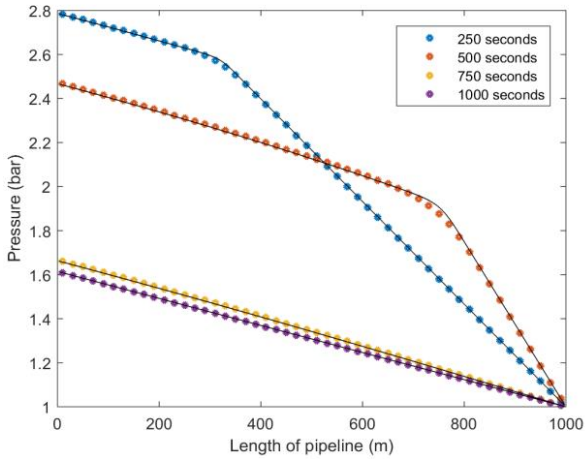

Figure 5 - Pressure profile at different times.

gases allow the software to simulate other drilling scenarios such as Wait & Weight or Driller's Method (during a well control scenario), UBD, pressurized mud cap drilling or cementing.

In this paper, an actual deviated offshore well was selected to better mimic a real-life scenario. The wellbore path (true vertical depth (TVD) vs. horizontal departure) is shown in **Figure 6**. **Table 1** summarizes additional information for this wellbore, including the drill string and annulus information.

Simulating Wait and Weight Method

In this section, a gas influx was introduced 3 min after the simulation started. The Wait & Weight Method was subsequently applied to cease and circulate out the kick. The simulation event timeline was as follows:

- **0-3 min:** Normal operation. Blowout preventer was open. Drilling fluid flow-in rate was set to 500 gal/min. The original mud had a weight of 11.8 ppg, yield stress of 5 Pa, fluid behavior index of 0.6 and consistency index of 0.2 Pa.s.$^{0.6}$

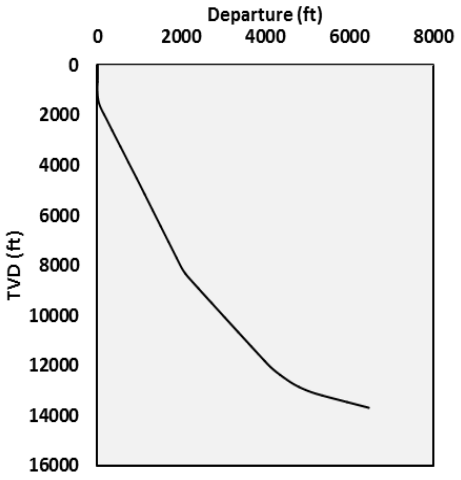

Figure 6 - Wellbore path (TVD vs. horizontal departure).

Table 1 - Drill string and annulus data for the offshore well.

Property	Value
Pipe OD, ID, length	5.875", 5.153", 15188 ft
Heavy Wall Drill pipe OD, ID, length	5.875", 4", 569 ft
Drill collars OD, ID, length	6.5625", 3.0625, 90 ft
Annulus Section 1 (casing 1), ID and length	9.56 inch, 6200 ft
Annulus Section 1 (casing 2), ID and length	9.76 inch, 8365 ft
Annulus Section 3 (open hole), ID and length	9.5 inch, 1282 ft

- **3-7 min:** Reservoir pressure was set to be higher than the bottom hole pressure and gas influx occurred at the bottom of the well.
- **7-9 min:** Pump was stopped for flow check. Kick was detected.
- **9-50 min:** "Wait" Stage of the Wait & Weight Method. The well was shut in by closing the blowout preventer. Heavy mud was made, which has a weight of 12.6 ppg with yield stress of 10.06 Pa, fluid behavior index of 0.7323 and consistency index of 0.3285 Pa.s.$^{0.7323}$
- **50-340 min:** Heavy mud was pumped at a kill rate of 200 gal/min. At the same time, a standard proportional-integral (PI) controller was applied to keep the bottom-hole pressure constant during circulation.

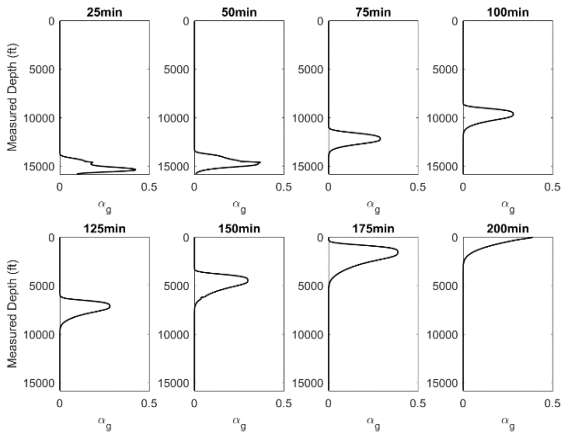

Figure 7 - Gas void fractions vs. measured depth at different times during Wait & Weight Method.

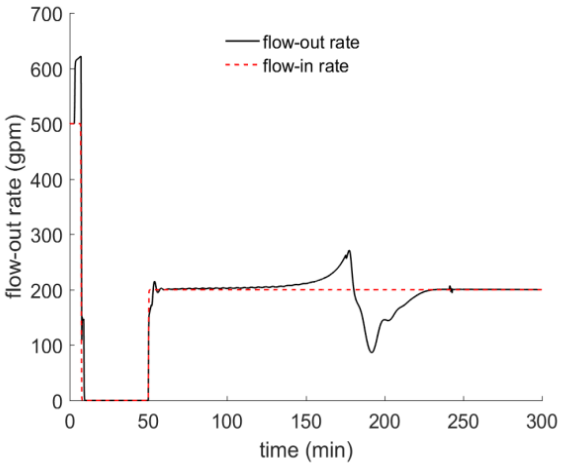

Figure 8 - Flow in/out rate vs. time during Wait & Weight Method.

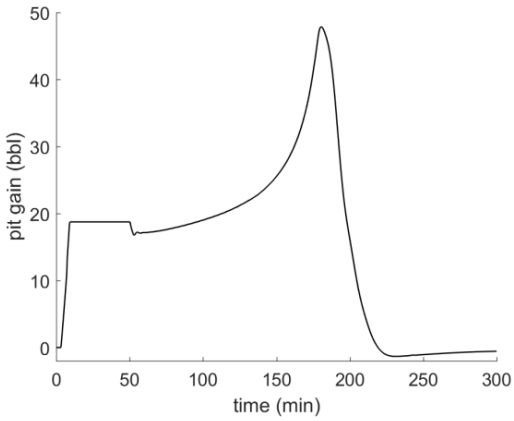

Figure 9 - Pit gain vs. time during Wait & Weight Method.

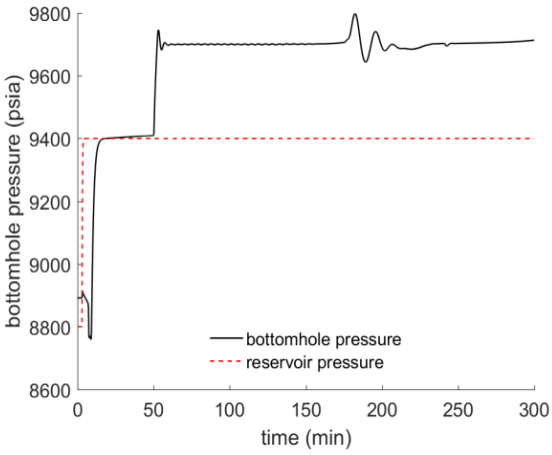

Figure 10 - Bottom-hole pressure vs. time during Wait & Weight Method.

Figure 7 shows the gas void fractions vs. time while removing the gas kick from the wellbore. Gas reached the surface after 180 min. As shown in **Figure 7** , the flow out rate increased once the gas kick was initiated due to the pressure difference between reservoir pressure and bottom-hole pressure. As a result, the pit gain was also increased as shown in **Figure 9**, which presented an additional indicator for this gas kick. A flow check was subsequently conducted by stopping the mud pump and checking the flow-out rate. The gas kick was confirmed by observing non-zero flow-out rate after the mud pump was stopped. Once the kick was confirmed, the well was shut in immediately followed by a 41-min stage for making the heavy mud. During the subsequent pumping stage starting at 50 min, the heavy mud was pumped at a kill rate of 200 gal/min until the kick was circulated out.

Figure 10 shows the bottom-hole pressure vs. time during the gas kick event. Initially, bottom-hole pressure slightly increased due to the additional frictional pressure drop introduced by gas entrance. Then, when the gravitational pressure gradient became dominant, a decrease in the bottom-hole pressure was observed. Subsequently, the well was shut in to increase the bottom-hole pressure and stop the influx. During the "Wait" stage, flow in and out rates were zero. Gas rose slowly due to slip between the liquid and gas velocities. The gas expansion caused a slight increase of the casing pressure and thus the bottom-hole pressure. During the pumping stage, an automated choke was applied to keep the bottom-hole pressure constant and approximately 300 psi above the reservoir pressure.

Figure 11 shows the surface backpressure vs. time during the gas kick event. Peak casing pressure (approximately 1300 psi) was observed when the influx reached the surface. As heavy mud replaced the original mud in the wellbore, the surface backpressure dropped back to atmospheric pressure. This indicated that the procedure was successful and no additional kick was taken during circulation.

Figure 12 shows the standpipe pressure vs. time during the gas kick event. The shut-in drill pipe pressure of approximately 800 psi was observed. This value was used to obtain the required density for the kill mud. The standpipe pressure dropped as the original mud was replaced by the heavy mud in the drill string. It remained nearly constant when the mud in the

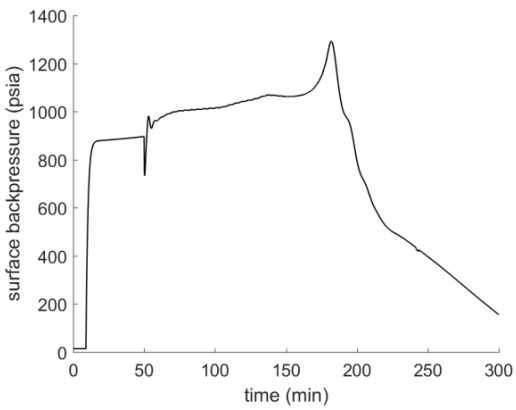

Figure 11 - Surface backpressure vs. time during Wait & Weight Method.

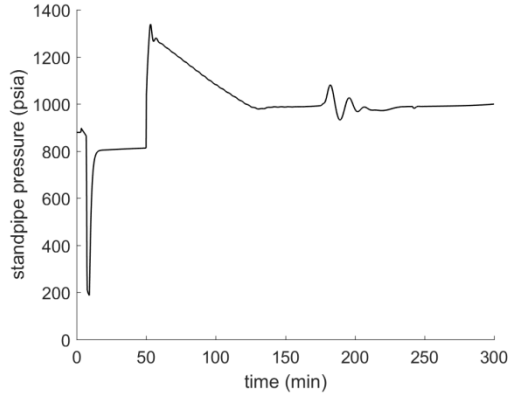

Figure 12 - Standpipe pressure vs. time during Wait & Weight Method.

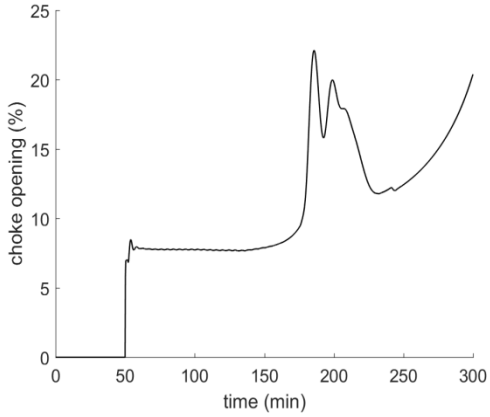

Figure 13 - Choke opening vs. time during Wait & Weight Method.

wellbore was replaced. **Figure 13** shows the choke opening vs. time during the gas kick event. Applying appropriate choke control algorithm was crucial to avoid significant oscillations in bottom-hole pressure during removal of the gas influx.

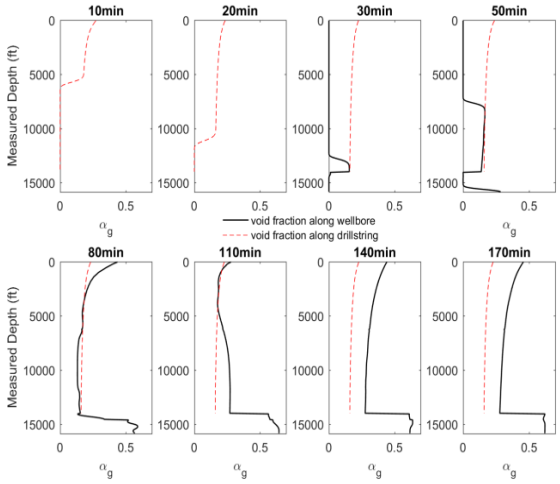

Figure 14 - Gas void fractions vs. measured depth inside the drill string (red line) and annulus (black line) at different times during UBD.

Simulating Underbalanced Drilling

In this section, drilling with an aerated fluid and off-bottom drill string is simulated. Nitrogen was injected to the drill string at the surface to induce the under-balanced conditions in the wellbore. After nitrogen reached the bit, the bottom-hole pressure gradually fell below the reservoir pressure, which introduced a gas influx from the productive zone (which is assumed to be located at the bottom of the well). The same wellbore and drill string parameters in Table 1 were used, except that the drill string was 1847 ft off-bottom when the gas injection began at the surface. The simulation event timeline was as follows:

- **0-60 min:** Drilling fluid injection rate was set to 500 gal/min. The mud was a Newtonian fluid with a weight of 8.34 ppg and a constant viscosity of 1cP. Nitrogen was injected from the top of drill string at a rate of 4000 scfm. Choke opening was set to 40% to achieve a surface backpressure of 200 psi.
- **60-200 min:** An automated choke was applied to keep the bottom-hole pressure constant and below the reservoir pressure for underbalanced drilling.

Figure 14 shows the gas void fractions along wellbore and annulus vs. time during the underbalanced drilling. Injected gas reached the bit around 25 min and reached the surface around 70 min. As shown in **Figure 16**, the bottom-hole pressure fell below the reservoir pressure after approximately 45 min and introduced an influx at the bottom-hole location. The gas influx from the formation subsequently traveled upward and mixed with the injected gas from the drill string, which was 1847 ft above the bottom-hole location. This explained the high gas void fraction below the bit in the annulus after the gas influx occurred. Note that this process was time-dependent. Hence, applying steady-state multi-phase models/correlations may lead to erroneous results. The liquid flow in/out rate, bottom-hole

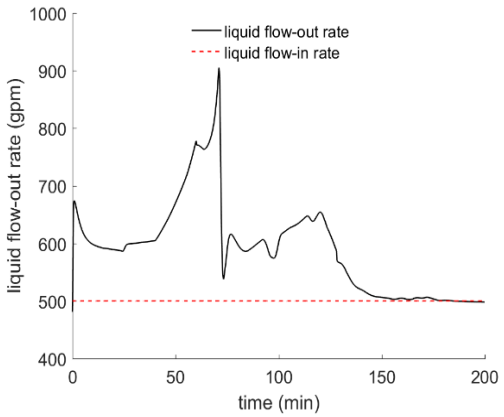

Figure 15 – Liquid flow in/out rate vs. time during UBD.

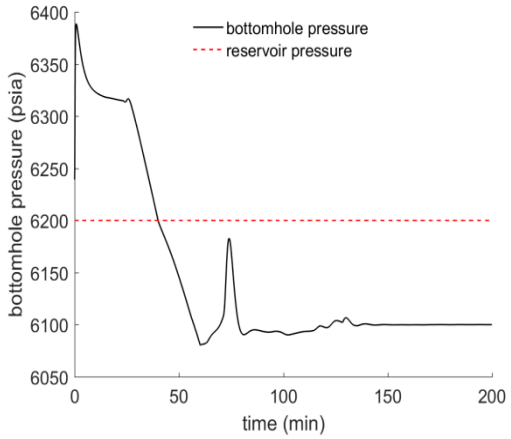

Figure 16 - Bottom-hole pressure vs. time during Underbalanced Drilling.

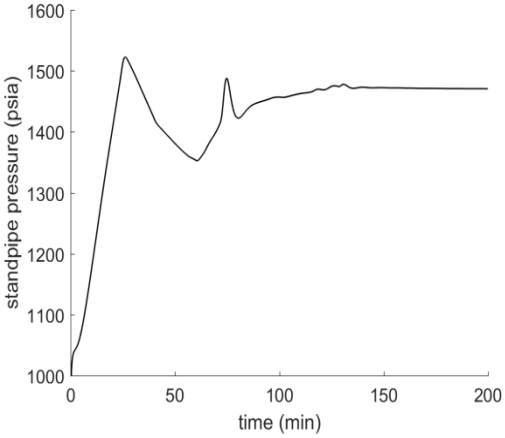

Figure 17 - Standpipe pressure vs. time during Underbalanced Drilling.

pressure, standpipe pressure, and choke opening during underbalanced drilling are shown in **Figure 15** through **18**, respectively.

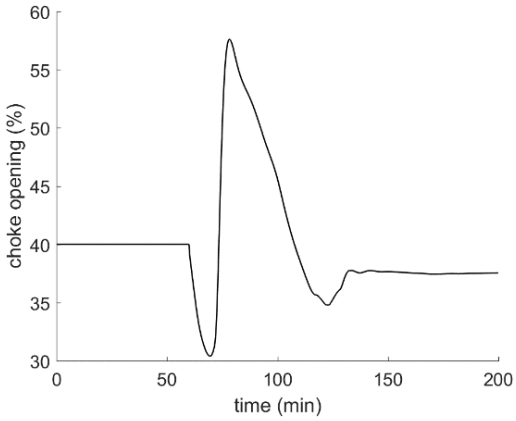

Figure 18 – Choke opening vs. time during Underbalanced Drilling.

Operating the choke is one of the crucial parameters during the UBD operations due to slow transients associated with multi-phase flow. Therefore, this software package can be used to evaluate and optimize the choke performance by comparing different choke models.

Conclusions

In this paper, a novel transient multi-phase flow modeling framework is proposed. It is based on the drift flux model with coupled conservation equations of mass, momentum, and energy in association with appropriate closure algebraic equations. Comprehensive slip laws, area discontinuities, arbitrary well path, non-Newtonian drilling fluids, nonlinear density models are all incorporated to improve the modeling accuracy. A second order semi-implicit numerical scheme is developed to efficiently and accurately solve the mathematical model. The developed model is validated by using previously published data. The proposed modeling framework is capable of simulating different drilling scenarios including conventional well control, UBD, MPD, dynamic well control, single-phase flow, etc.

In this study, the software package was used to simulate a conventional well control scenario as well as a UBD case. The proposed modeling framework is able to accurately estimate crucial parameters during hydraulic planning such as annular pressure profile, ECD, kick tolerance, flow out, pit gain, gas rising velocities etc. The model has been implemented in a user-friendly software package, which has the potential of facilitating hydraulic planning, enhancing rig safety, and reducing non-productive time due to well control-related issues.

Acknowledgment

We would like to thank Baker Hughes for financial support for this project and also for their help, encouragement and expert guidance during software development. The members of the Rig Automation and Performance Improvement in Drilling (RAPID) group at The University of Texas at Austin are thanked for their support and assistance through this study.

Nomenclature

A_c= Choke area, m^2

C_0 = Profile parameter, m^2

f_G = Gravitational pressure drop, Pa/m

f_w = Frictional pressure drop, Pa/m

g = Gravitational constant, m/s^2

p_0 = Atmospheric pressure, Pa

p_{bh} = Bottom-hole pressure, Pa

p_{ds} = Choke downstream pressure, Pa

p_{res} = Reservoir pressure, Pa

p_{top} = Surface backpressure, Pa

q_c = Total mass flow through choke, kg/s

v_d = Drift velocity, m/s

v_g = Gas velocity, m/s

v_l = Liquid velocity, m/s

v_{mix} = Mixed velocity of gas and liquid, m/s

$x_{g,top}$= Gas mass flow fraction through choke

$x_{l,top}$ = Liquid mass flow fraction through choke

Y = Gas expansion factor

Z_c = Choke opening

α_g= Gas volume fraction

α_l= Liquid volume fraction

ρ_g= Gas density, kg/m^3

ρ_l= Liquid density, kg/m^3

$\rho_{l,0}$ = Reference liquid density, kg/m^3

ρ_{mix} = Mixed density of gas and liquid, kg/m^3

μ_l= Liquid viscosity, Pa.s

μ_g= Gas viscosity, Pa.s

μ_{mix}= Mixed viscosity of gas and liquid, Pa.s

γ = Adiabatic index of gas

θ = Well inclination angle from vertical, rad

Δp_c = Choke critical pressure drop ratio

Glossary

ECD = *Equivalent circulating density*
MPD = *Managed pressure drilling*
TVD = *True vertical depth*
UBD = *Under-balanced drilling*
YPL = *Yield power law*

References

Aarsnes, U.J.F., Ambrus, A., Vajargah, A.K., Aamo, O.M., van Oort, E., 2015. A simplified gas-liquid flow model for kick mitigation and control during drilling operations, in: ASME 2015 Dynamic Systems and Control Conference. American Society of Mechanical Engineers, p. V002T20A002–V002T20A002.

Abouie, A., 2015. Development and application of a compositional wellbore simulator for modeling flow assurance issues and optimization of field production.

Abouie, A., Shirdel, M., Darabi, H., Sepehrnoori, K., 2015. Modeling asphaltene deposition in the wellbore during gas lift process, in: SPE Western Regional Meeting. Society of Petroleum Engineers.

Avelar, C.S., Ribeiro, P.R., Sepehrnoori, K., 2009. Deepwater gas kick simulation. J. Pet. Sci. Eng. 67, 13–22.

Beggs, D.H., Brill, J.P., 1973. A study of two-phase flow in inclined pipes. J. Pet. Technol. 25, 607–617.

Bendiksen, K.H., Maines, D., Moe, R., Nuland, S., 1991. The dynamic two-fluid model OLGA: Theory and application. SPE Prod. Eng. 6, 171–180.

Brill, J.P., 1985. Pressure drop correlations for inclined two-phase flow. J. Energy Resour. Technol. 107, 549.

Duns, H.J., Ros, N.C.J., 1963. Vertical flow of gas and liquid mixtures in wells. Presented at the 6th World Petroleum Congress, World Petroleum Congress.

Eaton, B.A., Knowles, C.R., Silberbrg, I.H., 1967. The prediction of flow patterns, liquid holdup and pressure losses occurring during continuous two-phase flow in horizontal pipelines. J. Pet. Technol. 19, 815–828.

Evje, S., Fjelde, K.K., 2002. Relaxation schemes for the calculation of two-phase flow in pipes. Math. Comput. Model. 36, 535–567.

Gavrilyuk, S.L., Fabre, J., 1996. Lagrangian coordinates for a drift-flux model of a gas-liquid mixture. Int. J. Multiph. Flow 22, 453–460.

Hagedorn, A.R., Brown, K.E., 1965. Experimental study of pressure gradients occurring during continuous two-phase flow in small-diameter vertical conduits. J. Pet. Technol. 17, 475–484.

Hasan, A.R., Kabir, C.S., 1998. A simplified model for oil-water flow in vertical and deviated wellbores, in: SPE Annual Technical Conference and Exhibition. Society of Petroleum Engineers.

Ma, Z., Vajargah, A.K., Ambrus, A., Ashok, P., Chen, D., van Oort, E., May, R., Macpherson, J.D., Becker, G., Curry, D.A., 2016. Multi-Phase Well Control Analysis During Managed Pressure Drilling Operations. Presented at the SPE Annual Technical Conference and Exhibition, Society of Petroleum Engineers. doi:10.2118/181672-MS

Nickens, H.V., 1987. A dynamic computer model of a kicking well. SPE Drill. Eng. 2, 159–173.

Oddie, G., Shi, H., Durlofsky, L.J., Aziz, K., Pfeffer, B., Holmes, J.A., 2003. Experimental study of two and three phase flows in large diameter inclined pipes. Int. J. Multiph. Flow 29, 527–558.

Podio, A.L., Yang, A.-P., 1986. Well control simulator for IBM personal computer, in: SPE/IADC Drilling Conference. Society of Petroleum Engineers.

Rommetveit, R., 1989. A Numerical Simulation Model for Gas-Kicks in Oil Based Drilling Fluids. PhD dissertation, University of Bergen, Norway.

Rommetveit, R., Vefring, E.H., 1991. Comparison of results from an advanced gas kick simulator with surface and downhole data from full scale gas kick experiments in an inclined well, in: SPE Annual Technical Conference and Exhibition. Society of Petroleum Engineers.

Roumazeilles, P.M., Yang, J., Sarica, C., Chen, X., Wilson, J., Brill, J.P., 1996. An experimental study on downward slug flow in inclined pipes. SPE Prod. Facil. 11, 173–178.

Shi, H., Holmes, J.A., Durlofsky, L.J., Aziz, K., Diaz, L., Alkaya, B., Oddie, G., 2005. Drift-Flux Modeling of Two-Phase Flow in Wellbores. SPE J. 10, 24–33. doi:10.2118/84228-PA

Shirdel, M., Sepehrnoori, K., 2012. Development of a transient mechanistic two-phase flow model for wellbores. SPE J. 17, 942–955.

Udegbunam, J.E., Fjelde, K.K., Evje, S., Nygaard, G., 2014. A simple transient flow model for mpd and ubd applications, in: SPE/IADC Managed Pressure Drilling & Underbalanced Operations Conference & Exhibition. Society of Petroleum Engineers.

Yuan, H., Zhou, D., 2009. Evaluation of Twophase Flow Correlations and Mechanistic Models for Pipelines at Horizontal and Inclined Upward Flow, in: SPE Production and Operations Symposium. Society of Petroleum Engineers.

Appendix

Slip Law (Continued)

For the simulation scenarios presented in this paper, the model proposed by Shi et al. (2005) was applied with parameter corrections for inclined flow (Hasan and Kabir, 1998):

$$\begin{cases} C_0 = \dfrac{A}{1+(A-1)\gamma} \\ v_d = \dfrac{(1-\alpha_g C_0)C_0 K(\alpha_g) v_c}{\alpha_g C_0\sqrt{\rho_g/\rho_l} + 1 - \alpha_g C_0}\sqrt{\cos(\theta)}\,[1+\sin(\theta)]^2 \end{cases} \quad \text{(A1)}$$

where $A, \gamma, K(\alpha_g), v_c$ are empirical parameters, $\alpha_g = \sum_{k=1}^{K}\alpha_{g,k}$ is the volume fraction of gas phase, $\rho_g = \left(\sum_{k=1}^{K}\alpha_{g,k}\rho_{g,k}\right)/\alpha_g$ and $\rho_l = \left(\sum_{i=1}^{I}\alpha_{l,i}\rho_{l,i}\right)/(1-\alpha_g)$ are the densities of gas and liquid phases, respectively. θ denotes the inclination angle from the vertical.

Choke Model

Adding backpressure in well control is conducted by adjusting the choke opening. For the stratified flow, the following choke model is used (Aarsnes et al., 2015):

$$\begin{cases} q_c = \dfrac{A_c Z_c\sqrt{2\max(p_{top}-p_{ds},\ 0)}}{\sum_{i=0}^{I}\left(x_{l,i,top}/\sqrt{\rho_{l,i,top}}\right) + \sum_{k=0}^{K}\left(x_{g,k,top}/\left(Y_k\sqrt{\rho_{g,k,top}}\right)\right)} \\ x_{l,i,top} = \left[\dfrac{\alpha_{l,i}\rho_{l,i}v_l}{\sum_{i=0}^{I}(\alpha_{l,i}\rho_{l,i})v_l + \sum_{k=0}^{K}(\alpha_{g,k}\rho_{g,k})v_g}\right]_{top} \\ x_{g,k,top} = \left[\dfrac{\alpha_{g,k}\rho_{g,k}v_g}{\sum_{i=0}^{I}(\alpha_{l,i}\rho_{l,i})v_l + \sum_{k=0}^{K}(\alpha_{g,k}\rho_{g,k})v_g}\right]_{top} \\ Y_k = 1 - \dfrac{p_{top}-p_{ds}}{3p_{top}\Delta p_c\gamma_k/1.4} \end{cases} \quad \text{(A2)}$$

where q_c, A_c, Z_c, p_{top}, p_{ds} and Δp_c are the total mass flow rate through the choke, choke area, choke opening in percentage, surface back pressure, choke downstream pressure, and critical pressure drop ratio, respectively. $x_{l,i,top}$ and $\rho_{l,i,top}$ are the mass flow fraction and density of the i^{th} liquid component at the surface. $x_{g,k,top}$, $\rho_{g,k,top}$, γ_k and Y_k are the mass flow fraction, density, adiabatic index and gas expansion factor of the k^{th} gas component at the surface. For a mixed flow region such as bubble flow or dispersed bubble flow, equation (A2) is modified as follows:

$$q_c = A_c Z_c\sqrt{\frac{2\max(p_{top}-p_{ds},\ 0)}{\sum_{i=0}^{I}\left(x_{l,i,top}/\rho_{l,i,top}\right) + \sum_{k=0}^{K}\left(x_{g,k,top}/\left(Y_k^2\rho_{g,k,top}\right)\right)}} \quad \text{(A3)}$$

The mass flow rate through the choke for liquid or gas can be calculated as the product of the total mass flow rate (q_c) and the corresponding mass flow fraction ($x_{l,i,top}$ or $x_{g,k,top}$).